

We are IntechOpen, the world's leading publisher of Open Access books Built by scientists, for scientists

6,900

Open access books available

185,000

International authors and editors

200M

Downloads

Our authors are among the

154

Countries delivered to

TOP 1%

most cited scientists

12.2%

Contributors from top 500 universities



WEB OF SCIENCE™

Selection of our books indexed in the Book Citation Index
in Web of Science™ Core Collection (BKCI)

Interested in publishing with us?
Contact book.department@intechopen.com

Numbers displayed above are based on latest data collected.
For more information visit www.intechopen.com



Application of Fast Fourier Transform for Accuracy Evaluation of Thermal-Hydraulic Code Calculations

Andrej Prošek and Matjaž Leskovar
*Jožef Stefan Institute
 Slovenia*

1. Introduction

To study the behaviour of nuclear power plants, sophisticated and complex computer codes are needed. Before the computer codes are used for safety evaluations they have first to be validated. The assessment process of system codes involves the comparison of code results against experimental data and measured plant data. The accuracy of the code is the capability of the code to correctly predict the physical behaviour. Therefore the evaluation of accuracy coincides with code validation. In the past a few methods to quantify the code accuracy of thermal-hydraulic system codes have been proposed. Among the proposed methods, the approach using the fast Fourier transform has been proposed as one of the most effective approaches in 1990s (Ambrosini et al., 1990; D'Auria et al., 1994). The fast Fourier transform based method (FFTBM) shows the measurement-prediction discrepancies, i.e. the accuracy quantification, in the frequency domain. From the amplitudes of the component frequencies, the average amplitude (AA) is calculated. AA sums the difference between experimental and calculated signal discrete Fourier transform amplitudes at each frequency. To get a dimensionless accuracy measure, the sum of the amplitudes of the experimental signal is used for normalization. The closer the non-dimensional AA value is to zero, the better the agreement between the calculated results and the experimental measurements is judged. However, some problems involved in FFTBM, such as proper selection of time windows, weighting factors, number of discrete data used, consistency of the method in all cases and time dependent accuracy, still remain open and partly limit its application, especially those requiring a consistent accuracy judgement. For example, in early applications of FFTBM problems in evaluating signals, where experimental or error signal has the shape similar to triangle (i.e. first increases and then decreases), the accuracy value regularly overshoots at triangle peak, stabilising at lower value when discrepancy decrease (Mavko et al. 1997). Not being aware about the reasons of such or some other strange behaviour, the FFTBM method has been also criticized. In general it is required that at any time into the transient the accuracy measure should remember the previous history. But on the other hand, the original FFTBM method has been effectively applied in obtaining information on code accuracy by several researchers in the literature. More recently, an automated code assessment program (ACAP) has been developed to provide a quantitative comparison between nuclear reactor system code results and

experimental measurements (Kunz et al., 2002). For the time record data the original FFTBM accuracy measure was modified and a new continuous wavelet transformation accuracy measure was included among several other accuracy measures developed for timing of events tables, scatter plots and steady state data. Unfortunately, the ACAP tool was developed for single variable comparison only. Besides, not many measures were effective in evaluating time record data. This means that the original FFTBM remained in use. In 2002, the review of important applications was done (Prošek et al., 2002). Much of the work was performed mostly in the application domain. The comparisons between the experimental data and calculated results were done for different transients and accidents on different experimental facilities. The first large FFTBM application was to the international standard problem no. 27 (ISP-27) in which primary system thermal-hydraulic system codes were used (D'Auria et al., 1994) to the BETHSY facility simulating the French pressurized water reactor. The maturity was shown in that the method was sensible in highlighting the differences between pre- and post-test calculations for the same user, normally originating by an ad-hoc code tuning operated in post-test analyses and by the code use at the international level. The first application of FFTBM to containment code calculations was to ISP-35 performed on the NUPEC facility (D'Auria et al., 1995). The need for potential further efforts to refine the weighting factors was expressed. The application to ISP-39 performed on the FARO facility (D'Auria & Galassi, 1997) was the first application of FFTBM to severe accidents. The application confirmed the capabilities of the FFTBM method only in ranking generic calculation results. The application to ISP-42 performed on the PANDA facility (Aksan et al., 2001) showed that ten variables were not enough to completely characterize the transient. Finally, the application of FFTBM to the ISP-13 exercise, post-test calculations of the LOFT L2-5 test was performed in the frame of the BEMUSE program (OECD/NEA, 2006). The original FFTBM approach was used in this application. The numerous applications showed that there are some deficiencies of the original FFTBM, which were resolved in the proposed improved FFTBM.

In this Chapter, we first describe the original FFTBM approach. Then the time dependent accuracy measures are introduced. By calculating the time dependent accuracy it can be answered, which discrepancy contributes and how much is its contribution to the inaccuracy. Then, the index for time shift indication is proposed. The application of the time dependent accuracy showed that the original FFTBM gave an unrealistic judgment of the accuracy for monotonically increasing or decreasing functions, causing problems in FFTBM results interpretation. This problem was hidden in the past when FFTBM was applied only to a few time windows and/or intervals. It was found out that the reason for such an unrealistic calculated accuracy of increasing/decreasing signals is the edge between the first and last data point of the investigated signal, when the signal is periodically extended. Namely, if the values of the first and last data point of the investigated signal differ, then there are discontinuities present in the periodically extended signal seen by the discrete Fourier transform, which views the finite domain signal as an infinite periodic signal. The discontinuities give several harmonic components in the frequency domain, thus increasing the sum of the amplitudes, on which FFTBM is based, and by this influencing the accuracy. The influence of the edge due to the periodically extended signal is for clarity reasons called edge effect. It should be noted that the signal may include several other rising and falling edges, which influences are not considered as edge effect in this chapter. The quantitative contribution of the edge effect on the accuracy may be very unpredictable and can

overshadow the contribution of the discrepancies of the compared functions on the accuracy. Therefore it is proposed how to resolve the problem of the edge effect on a unique way by signal mirroring.

In order to demonstrate its application, the proposed improved FFTBM by signal mirroring is tested to show that it gives a realistic and consistent judgment of the accuracy also for monotonically increasing or decreasing functions, and for all other signals influenced by the edge effect. The results obtained with FFTBM results were compared to results obtained with ACAP. At the end general recommendations for applying FFTBM are given.

2. Original FFTBM description

The methodology of the code-accuracy assessment consists of three steps: a) selection of the test case (experimental or plant measured data to compare), b) qualitative analysis, and c) quantitative analysis. The qualitative analysis is a prerequisite to perform the quantitative analysis. The qualitative analysis, including visual observation of plots, is done by evaluating and ranking the discrepancies between the measured and calculated variable trends. The quantitative analysis (applying FFTBM) is meaningless unless all the important phenomena are predicted.

The original FFTBM is a method (Ambrosini et al., 1990), which shows the measurement-prediction discrepancies in the frequency domain. The method purpose is to quantify the accuracy of code calculations based on the amplitudes of the discrete experimental and error signal calculated by the fast Fourier transform (FFT). On the other hand, the digital computers can only work with information that is discrete and finite in length and there is no version of the Fourier transform that uses finite length signals (Smith, 1999). The way around this is to make the finite data look like an infinite length signal. This is done by imagining that the signal has an infinite number of samples on the left and right of the actual points. The imagined samples can be a duplication of the actual data points. In this case, the signal looks discrete and periodic. This calls for the discrete Fourier transform (DFT) to be used. There are several ways to calculate DFT. One method is FFT. While it produces the same results as the other approaches, it is incredibly more efficient. The key point to understand the FFTBM is that the periodicity is invoked in order to be able to use a mathematical tool, i.e., the DFT. Therefore, the periodic nature of DFT is explained first before the accuracy measures used in FFTBM are described.

2.1 Periodic nature of discrete Fourier transform

The discrete Fourier transform views both, the time domain and the frequency domain, as periodic (Smith, 1999). The signals used for comparison are not periodic. Nevertheless, the user must conform to the DFT's view of the world. Figure 1 shows two different interpretations of the time domain signal. In the upper part of Fig. 1 the time domain is viewed as N points. This represents how digital signals are typically acquired in experiments and code calculations. For instance, these 64 samples might have been acquired by sampling some parameters at regular intervals of time. Sample 0 is distinct and separate from sample 63 because they were acquired at different times. The samples on the left side are not related to the samples on the right.

As shown in the lower part of Fig. 1, the DFT views these 64 points to be a single period of an infinitely long periodic signal. This means that the left side of the signal is connected to the right side of a duplicate signal, and vice versa. The most serious consequence of time

domain periodicity is the occurrence of the edge. When the signal spectrum is calculated with DFT, the edge is taken into account, despite the fact that the edge has no physical meaning for comparison, since it was introduced artificially by the applied numerical method. It is known that the edge produces a variegated spectrum of frequencies due to the discontinuity of the edge. These frequencies originating from the artificially introduced edge may overshadow the frequency spectrum of the investigated signal.

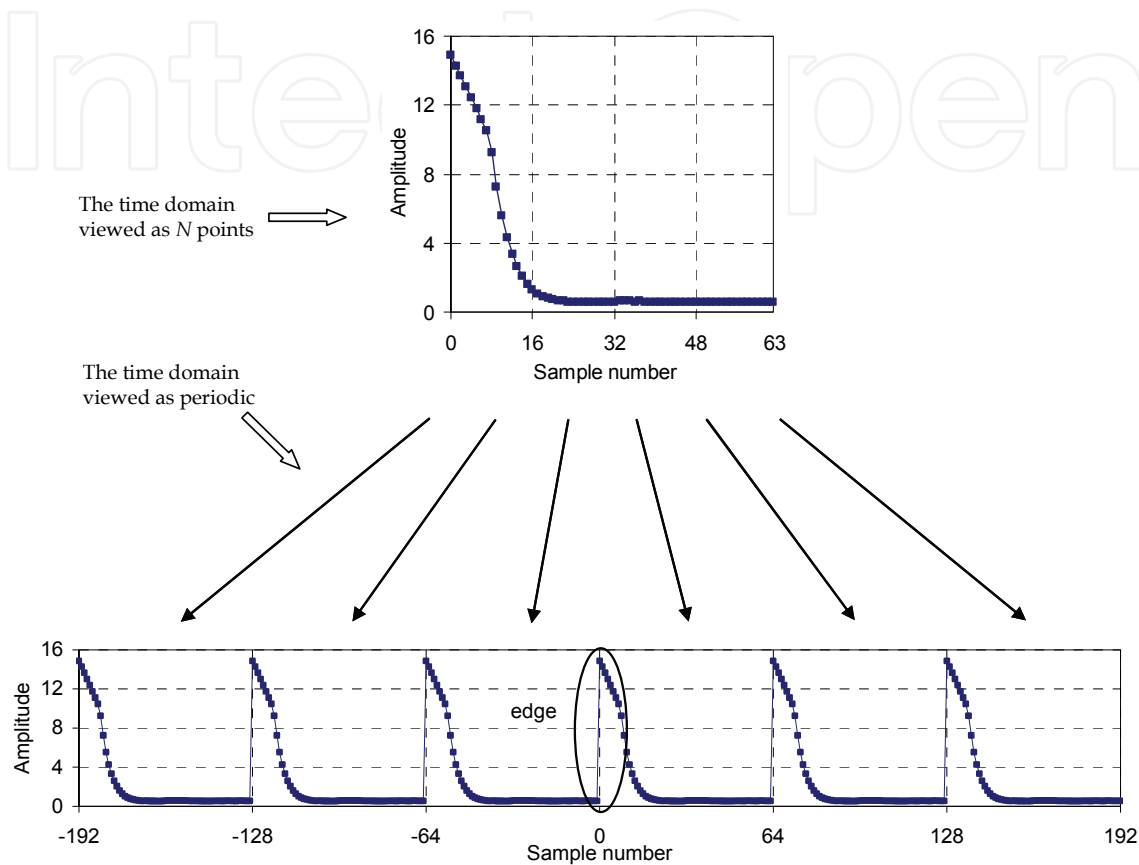


Fig. 1. Periodicity of the DFT's time domain original signal. The time domain can be viewed as N samples in length, shown in the upper part of the figure, or as an infinitely long periodic signal, shown in the lower part of the figure

2.2 Average amplitude

For the calculation of measurement-prediction discrepancies the experimental signal $F_{exp}(t)$ and the error signal $\Delta F(t)$ are needed. The error signal in the time domain is defined as $\Delta F(t) = F_{cal}(t) - F_{exp}(t)$ where $F_{cal}(t)$ is the calculated signal. The code accuracy quantification for an individual calculated variable is based on the amplitudes of the discrete experimental and error signal obtained by FFT at frequencies f_n , where $n = 0, 1, \dots, 2^m$ and m is the exponent defining the number of points $N = 2^{m+1}$. The average amplitude AA is defined:

$$AA = \frac{\sum_{n=0}^{2^m} |\tilde{\Delta F}(f_n)|}{\sum_{n=0}^{2^m} |\tilde{F}_{exp}(f_n)|}, \tag{1}$$

where $|\tilde{\Delta F}(f_n)|$ is the error signal amplitude at frequency f_n and $|\tilde{F}_{\text{exp}}(f_n)|$ is the experimental signal amplitude at frequency f_n . The AA factor can be considered a sort of average fractional error and the closer the AA value is to zero, the more accurate is the result. Typical values of AA are from 0 to 1.

2.3 Total average amplitude

The overall picture of the accuracy for a given code calculation is obtained by defining average performance index, that is the AA_{tot} (total average amplitude or total accuracy)

$$AA_{\text{tot}} = \sum_{i=1}^{N_{\text{var}}} (AA)_i \cdot (w_f)_i, \quad (2)$$

with

$$\sum_{i=1}^{N_{\text{var}}} (w_f)_i = 1, \quad (3)$$

where N_{var} is the number of the variables analyzed (typically from 20 to 25), and $(AA)_i$ and $(w_f)_i$ are the average amplitude and the weighting factor for the i -th analyzed variable, respectively. Each $(w_f)_i$ accounts for the experimental accuracy, the safety relevance of particular variables and its relevance with respect to the primary pressure. The weights must remain unchanged during each comparison between code results and experimental data concerning the same class of a transient (for more information on weighting factors see D'Auria et al., 1994). The acceptability factor for AA_{tot} was set to 0.4 and for primary system pressure to 0.1.

3. Time dependent accuracy

As mentioned in Section 2, the FFTBM methodology requires the qualitative assessment and the subdivision of the transient into phenomenological windows. Normally, the accuracy analysis is performed for time windows and time intervals, where each phenomenological window represents one time window, while time intervals start at the beginning of the transient and end at each phenomenological window end time.

Instead of a few phenomenological windows a series of narrow windows (phases) is proposed (around 40 windows / intervals for a transient). This gives the possibility to check the accuracy of each part of the transient and to get time dependency of accuracy measures. In the quantitative assessment with 3 to 5 phenomenological windows only global trends were available. In the present analysis by the term moving time window a set of equidistant narrow time windows as we progress into the transient is meant (like a moving chart strip). By the term increasing time interval a set of time intervals each increased for the duration of one narrow time window is meant, where the last time interval is equal to the whole transient duration time. The moving time window shows instantaneous details of $\Delta F(t)$ and consequently cannot draw an overall judgement about the accuracy, but focuses the analysis only on instantaneous discrepancies. An integral approach is needed to draw an overall judgement about accuracy and this is achieved by increasing the time interval, what also

shows how the accuracy changes with time progression. From these time dependant accuracy measures it can be easily seen when the largest total discrepancy occurs and what is its influence on the total accuracy. They also show how the transient duration selected for the analysis influences the results.

In Fig. 2 are shown the results for the three different participants using different computer codes for the standard problem exercise no. 4 (SPE-4) (Szabados et al., 2009), simulating the small-break loss of coolant accident on the PMK-2 facility.

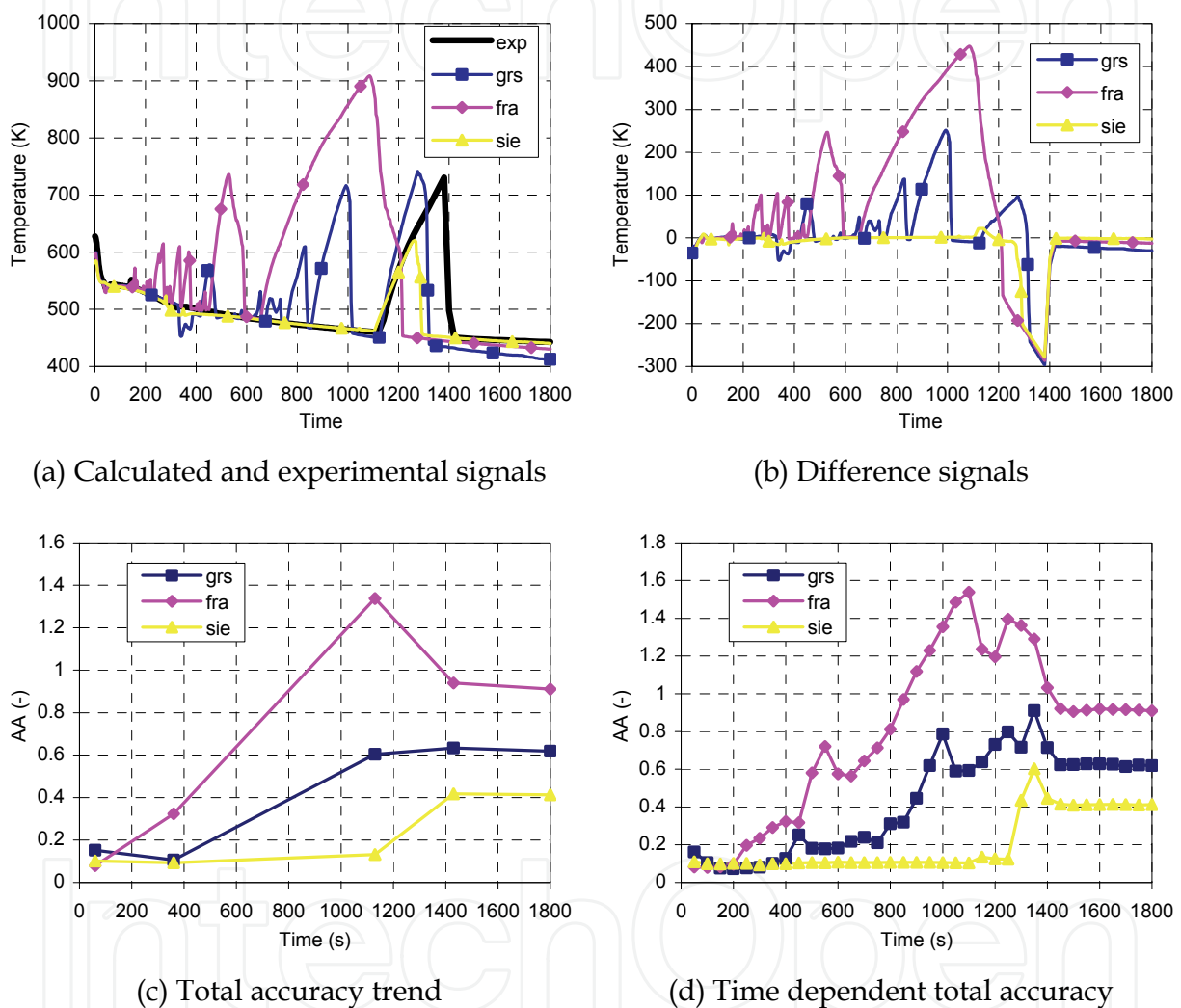


Fig. 2. Results for SPE-4 test calculations of rod surface temperature

The PMK-2 facility is the first integral type facility for VVER-440/213 plants. In the study by Szabados et al., 2009 the results for the signals are plotted (see Fig. 2(a)) and the accuracy for five selected time windows is given (see Fig. 2(c)). Figure 2(b) shows the difference signals, which are used for the AA calculation beside the experimental signal used for the normalization. Finally, Fig. 2(d) shows the AA calculated for increasing time intervals (each time 10 s), thus obtaining time dependent AA. When comparing Figs. 2(c) and 2(d) the contribution of discrepancies is better evident from Fig. 2(d). Also it can be seen how the accuracy overshoots due to edge effects, later stabilizing at some lower value.

4. Index for time shift detection

It should be noted that the AA accuracy measure (Equation 1) is not obtained by comparing the experimental and calculated magnitude spectra, but by calculating the magnitude spectrum of the difference signal. Nevertheless, due to the Fourier transform properties the magnitude spectrum of the difference signal can also be obtained by adding the experimental and calculated signal magnitude spectra (actually subtraction); they must be converted into a rectangular notation, added, and then reconverted back to a polar form. When the spectra are in a polar form, they cannot be added by simply adding the magnitudes and phases. The error function amplitude spectrum $|\tilde{\Delta}F(f_n)|$ can be expressed as:

$$\begin{aligned} |\tilde{\Delta}F(f_n)| &= |\tilde{F}_{exp}(f_n) - \tilde{F}_{cal}(f_n)| = \\ &= \sqrt{\left(\text{Re}(\tilde{F}_{exp}(f_n) - \tilde{F}_{cal}(f_n))\right)^2 + \left(\text{Im}(\tilde{F}_{exp}(f_n) - \tilde{F}_{cal}(f_n))\right)^2} = \\ &= \sqrt{M_1^2 + M_2^2 - 2M_1M_2(\cos\varphi_1\cos\varphi_2 + \sin\varphi_1\sin\varphi_2)}, \end{aligned} \quad (4)$$

where $\tilde{F}_{exp} = M_1 \cos\varphi_1 + iM_1 \sin\varphi_1$ and $\tilde{F}_{cal} = M_2 \cos\varphi_2 + iM_2 \sin\varphi_2$ (rectangular form).

This example shows that to calculate the difference magnitude spectrum we need both the magnitude and the phase of the experimental and calculated spectra. Information about the shape of the time domain signal is contained in the magnitude and in the phase. In other words, comparing the shapes of the time domain signals is done through calculating the difference signal magnitude spectrum. At the time of the development of the original FFTBM (Ambrosini et al., 1990) it was mentioned that a possible improvement of the method could involve “the development of the procedure taking into account the information represented by the phase spectrum of the Fast Fourier Transform in the evaluation of accuracy”. As we can see from Equation 4, the difference signal magnitude inherently includes the magnitude and the phase of the experimental and calculated signal. The finding that both, the magnitude and the phase of the experimental and calculated frequency spectra are contained in AA by making the Fourier transform of the difference signals is very important as this gives the possibility to compare the shapes of the signals. The authors agree with Smith et al., 1999 that it is difficult to imagine which information is contained in the phase spectrum of the difference signal, since the experimental and calculated phase cannot be simply added. Therefore, to the authors’ opinion the difference signal phase information is not applicable for the comparison of two signals. In the following, AA will be referred to as $AA^{M\varphi}$, since it contains the magnitude M and phase φ information.

The original FFTBM package allows time shifting of data trends to analyze separately the effects of delayed or anticipated code predictions concerning some particular phenomena or systems interventions. It is a Fourier transform property that a shift in the time domain corresponds to a change in the phase. This property was used to identify the signals which differ in the time shift. Namely, the magnitudes of such signals are the same and only their phases are different. Therefore, the following expression, not taking into account the phase, is proposed (Prošek & Leskovar, 2009):

$$AA^M = \frac{\sum_{n=0}^{2^m} \left| \tilde{F}_{exp}(f_n) - \tilde{F}_{cal}(f_n) \right|}{\sum_{n=0}^{2^m} \left| \tilde{F}_{exp}(f_n) \right|}, \quad (5)$$

where:

$$\begin{aligned} \left| \tilde{F}_{exp}(f_n) - \tilde{F}_{cal}(f_n) \right| &= \\ &= \left| \left(\left(\operatorname{Re}(\tilde{F}_{exp}(f_n)) \right)^2 + \left(\operatorname{Im}(\tilde{F}_{exp}(f_n)) \right)^2 \right)^{1/2} - \left(\left(\operatorname{Re}(\tilde{F}_{cal}(f_n)) \right)^2 + \left(\operatorname{Im}(\tilde{F}_{cal}(f_n)) \right)^2 \right)^{1/2} \right| = \\ &= |M_1 - M_2| = \sqrt{(M_1 - M_2)^2}. \end{aligned} \quad (6)$$

When $\varphi_1 = \varphi_2$, Equation 4 is equal to Equation 6. This means that expression AA^M is a measure containing information from magnitudes M only. It is known that when two signals are only time shifted, the magnitude spectra are the same and the value of AA^M is consequently zero. It is very unlikely that a calculated signal, which is not shifted, would have a shape giving the same magnitudes as the experimental signal, as the predictions are required to be qualitatively correct. Therefore, AA^M can be used to establish the value by which $AA^{M\varphi} \equiv AA$ is increased due to the time shift contribution. In $AA^{M\varphi}$, the information from both, the shape of the time domain signal and the time shift, is provided, while in AA^M , only the time invariant information of the time domain signal is provided, what can be regarded to a certain degree as the shape of the time domain signal. Therefore, the difference $AA^\varphi = AA^{M\varphi} - AA^M$ gives the information about the time shift contribution. This difference is further normalized to:

$$I = \frac{AA^{M\varphi} - AA^M}{AA^M} = \frac{AA^\varphi}{AA^M}, \quad (7)$$

where the indicator I tells how the compared time signals are shifted, and is therefore called the time shift indicator. The larger the value of the time shift indicator I , the larger is the contribution of the time shift to $AA^{M\varphi}$ of the difference signal. A large value of I ($I > 1$) indicates that the compared signals are maybe shifted in time. When $I > 2$, we can be quite confident into time shift.

5. Signal mirroring

Since the original FFTBM is based on the sum of the amplitudes of the frequency spectrum of the investigated signal, the frequencies originating from the artificially introduced edge may significantly contribute to the sum of the frequency spectrum amplitudes of the investigated signal. Consequently the accuracy measure based on the original FFTBM is significantly influenced by the edge and therefore does not present a consistent accuracy measure of the signals being compared. This inconvenient drawback of the original FFTBM may be completely cured by eliminating the artificially numerically introduced edge. This may be efficiently done by signal mirroring, where the investigated signal is mirrored before the FFTBM is applied.

5.1 Symmetrised signal

If we have a function $F(t)$, where $0 \leq t \leq T_d$ and T_d is the transient time duration, its mirrored function is defined as $F_{mir}(t) = F(-t)$, where $-T_d \leq t \leq 0$. From these two functions a new function is composed which is symmetrical around T_d : $F_m(t)$, where $0 \leq t \leq 2T_d$. By composing the original signal and its mirrored signal, a signal without an edge between the first and the last data sample is obtained when periodically extended, and is called symmetrised signal. The symmetrised signal is shown in Fig. 3. The upper figure shows the finite length signal and the lower figure shows the infinite length periodic signal.

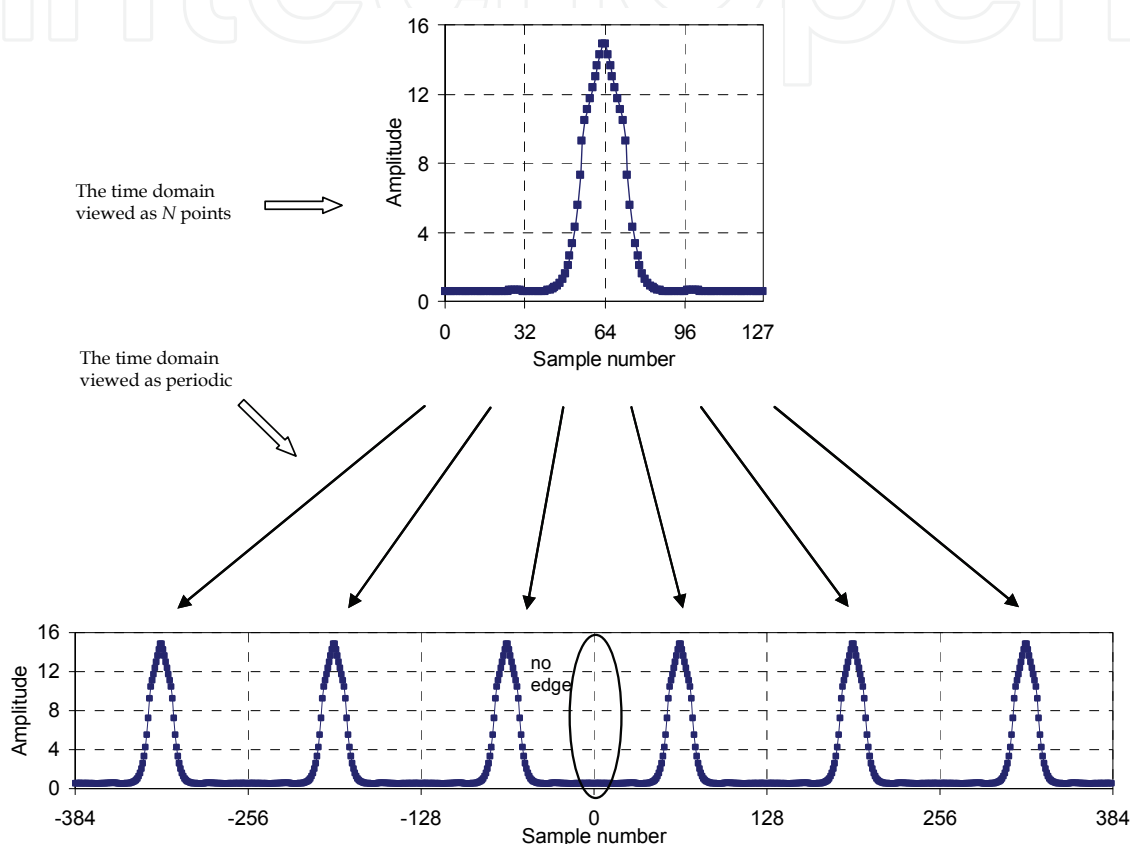


Fig. 3. Periodicity of the DFT's time domain symmetrised signal. The time domain can be viewed as N samples in length, shown in the upper part of the figure, or as an infinitely long periodic signal, shown in the lower part of the figure. We see that the symmetrised signal has no edge also when viewed as a periodic signal. Therefore in the sum of the frequency spectrum amplitudes only the amplitudes of the investigated signal are considered, as it should be. The FFTBM using the symmetrised signal is called "improved FFTBM by signal mirroring"

5.2 Deficiency of original FFTBM

When the original accuracy measures were proposed (Ambrosini et al., 1990) it seems that the impact of the edge effect was not considered. It is evident that this is a deficiency if the accuracy measure depends on the unphysical edge resulting from the intrinsic property of the DFT mathematical method, which treats the investigated finite length signal as an infinite length periodic signal. Namely, for the comparison the shape of the finite discrete

signal is important and not its edge characteristics. Also the visual comparison of signals is done in such a way.

It was already mentioned that the periodicity is invoked in order to use a mathematical tool. Therefore this influence should be eliminated. This was done by signal mirroring. When DFT is applied to the finite length symmetrised time domain signal the edge effect is obviously not introduced anymore.

5.3 Calculation of AA_m

For the calculation of the average amplitude by signal mirroring (AA_m) Equation 1 is used as for the calculation of AA , except that, instead of the original signal, the symmetrised signal is used. The reason to symmetrise the signal was to exclude the artificial edge from the signal without influencing the characteristics of the investigated signal. The signal is automatically symmetrised in the computer program for the improved FFTBM by signal mirroring (updated version of software described in Prošek & Mavko, 2003).

As already mentioned, the edge has no physical meaning for comparison, since it was introduced artificially by the applied numerical method, but FFT produces harmonic components because of it. By mirroring, the shapes of the experimental and error signal are symmetric and their spectra are different from the original signals spectra, mainly because they are without unphysical edge frequency components. Due to different spectra the sum of the amplitudes changes in both, the numerator and the denominator of Equation 1. To further demonstrate this in Sections 6.2 and 6.3, two new definitions are introduced for the average amplitude of the error signal (AA_{err}) and the average amplitude of the experimental signal (AA_{exp}), related with the numerator and denominator of Equation 1:

$$AA_{err} = \frac{1}{2^m + 1} \sum_{n=0}^{2^m} |\tilde{F}(f_n)|, \quad (8)$$

$$AA_{exp} = \frac{1}{2^m + 1} \sum_{n=0}^{2^m} |\tilde{F}_{exp}(f_n)|. \quad (9)$$

It should be noted that also when both, the original and error signal are without the artificial edge, in principal different AA_{err} and AA_{exp} may be obtained with the original FFTBM and the improved FFTBM by signal mirroring. Indeed AA and AA_m are slightly different measures also if the signals are without an artificial edge. The values obtained with the original FFTBM and the improved FFTBM by signal mirroring are the same only for symmetrical original signals. But this is not really a deficiency of the proposed improved FFTBM by signal mirroring, since it is important only that the method judges the accuracy on a realistic and unbiased way and that it is consistent within itself. In Section 6.4 it is presented how the accuracy calculated with the improved FFTBM by signal mirroring can be directly compared to the accuracy calculated with the original FFTBM.

6. Demonstration application

In this section some results are shown to see the advantages of the improved FFTBM by signal mirroring compared to the original FFTBM. First the test and the calculations used in the demonstration application of the improved FFTBM by signal mirroring are briefly

described. Then two case studies are presented. The case 1 study is presented to show how the artificial edge (when present) always changes the accuracy even if this is logically not expected. In the case 2 study the accuracy of one variable is calculated for two time windows. Average amplitudes of the error and experimental signal are calculated to show the impact of the edge effect. Finally, the improved FFTBM by signal mirroring is applied to LOFT L2-5 calculations performed in the frame of the Best-Estimate Methods Uncertainty and Sensitivity Evaluation (BEMUSE) Phase II to further show that the improved FFTBM by signal mirroring is more consistent in the quantitative assessment than the original FFTBM.

6.1 Test description

The LOFT L2-5 test was selected for this demonstration because the huge amount of data was available and the assessment of these test results with the original FFTBM was already published in the literature (OECD/NEA, 2006). The calculations of the LOFT L2-5 test, which is the re-analysis of the ISP-13 exercise, were performed in the phase II of the BEMUSE research program. The nuclear LOFT integral test facility is a scale model of a pressurized water reactor (OECD/NEA, 2006). The objective of the ISP-13 test was to simulate a loss of coolant accident (LOCA) caused by a double-ended, off-shear guillotine cold leg rupture coupled with a loss of off-site power. The experiment was initiated by opening the quick opening blowdown valves in the broken loop hot and cold legs. The reactor scrammed and emergency core cooling systems started their injection. After initial heatup the core was quenched at 65 s, following the core reflood. The LPIS injection was stopped at 107.1 s, after the experiment was considered complete. In total 14 calculations from 13 organizations were performed using 6 different codes (9 different code versions). The code most frequently used was RELAP5/MOD3.3. For more detailed information on the calculations the reader is referred to (OECD/NEA, 2006, Prošek et al., 2008).

6.2 Case 1 study by signal mirroring

To demonstrate how signal mirroring works, FFT was applied to the signals shown in Figs. 1 and 3. The AA_{exp} values of signals were calculated per Equation 9. Imagine that you would quantitatively assess two variables, with the shape of the experimental signals as shown in Figs. 1 and 3. Most probably you would judge that the judgment based on FFTBM should be the same for both signals as the area below the curve is the same when normalized with the number of data samples (the area below the symmetrised curve is the double area of the original signal). Nevertheless, in the case of the original FFTBM different values of AA_{exp} are obtained (25.87 for the original signal and 16.29 for the symmetrised signal), while in the case of the improved FFTBM by signal mirroring the same results are obtained for AA_{exp} of the original and symmetrised signal (16.29). This means that both, the original FFTBM and the improved FFTBM by signal mirroring produce the same results when no artificial edge is present in the signal and when the signal is symmetrical. This example clearly shows that the original FFTBM is not consistent when an artificial edge is present in the signal.

The difference between the original FFTBM and the improved FFTBM by signal mirroring results mainly due to the unphysical edge introduced by the applied numerical method, and can be directly quantified. The AA_{exp} of the symmetrised signal has to be extracted from the AA_{exp} of the original signal. In our example this contribution is 9.58 ((25.87 - 16.29) = 9.58). This means that the AA_{exp} of the experimental signal (used in the denominator of Equation 1) is 37% smaller when the edge effect is not considered, what would increase the

value of accuracy measure AA for 59% in this example. This means that all integral variables (e.g. integrated break flow, ECCS injected mass) and variables dropping from the nominal to a low value (e.g. power, primary pressure during LOCA) exhibit lower AA values just because the artificially introduced unphysical edge is present in the experimental signal. This basically explains the, in general, very high accuracy of these integral variables (Prošek et al., 2002) in comparison to other variables and why the acceptability factor for primary pressure (D'Auria et al., 1994) (dropping during small break LOCAs) had to be set to the very low value 0.1 (for other parameters there is no need for a special criterion). The improved FFTBM by signal mirroring provides a realistic, unbiased and consistent judgment, since it eliminates the effect of the unphysical edge, which sometimes is present and sometimes not. For example, when comparing primary pressures, during blowdown the pressure is decreasing and so a huge edge is present (it significantly decreases AA calculated by the original FFTBM), while during a very small break the pressure may recover to normal pressure after the initial drop due to emergency core cooling injection and consequently there is no edge (the original FFTBM then calculates similar values of AA as the improved FFTBM by signal mirroring).

6.3 Case 2 study by signal mirroring

To further demonstrate how signal mirroring works, in the second example the pressurizer pressure accuracy of LOFT L2-5 test calculations (see Fig. 4) is calculated for two time intervals, the blowdown phase time interval (0-20 s) and the whole transient time interval (0 – 119.5 s), as shown in Tables 1 and 2, respectively. Both, the original FFTBM and the improved FFTBM by signal mirroring were used. For each calculation the values of the average amplitude of the error signal (see Equation 8) and the average amplitude per Equation 1 are shown with the corresponding average amplitude of the experimental signal (see Equation 9). It should be noted that two calculations (Cal3, Cal6) did not provide data for the whole transient time interval; therefore for them the quantitative assessment was not applicable.

To see the influence of the edge elimination, the ratios of average amplitudes of the error signal obtained by the original FFTBM and the improved FFTBM by signal mirroring are shown in Tables 1 and 2. Besides the ratios, average amplitudes of the error signal, average amplitudes of the experimental signal, average amplitudes and rank of average amplitudes

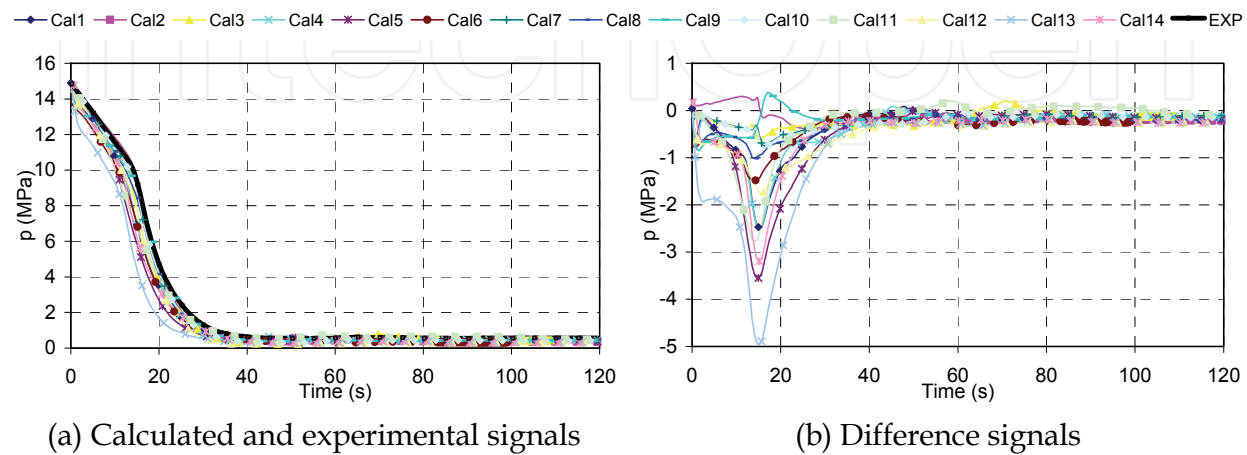


Fig. 4. Results of the LOFT L2-5 test for pressurizer pressure

| ID | AA _{err} | AA | AA _{err m} | AA _m | AA _{err} / AA _{err m} | Rank AA | Rank AA _m |
|-------|-------------------|-------|---------------------|-----------------|--|---------|-------------------------|
| Cal1 | 4.28 | 0.136 | 3.63 | 0.209 | 1.2 | 11 | 9 |
| Cal2 | 0.86 | 0.027 | 0.88 | 0.050 | 1.0 | 1 | 1 |
| Cal3 | 1.34 | 0.043 | 1.14 | 0.066 | 1.2 | 2 | 2 |
| Cal4 | 4.13 | 0.131 | 3.64 | 0.209 | 1.1 | 10 | 10 |
| Cal5 | 6.80 | 0.216 | 4.76 | 0.274 | 1.4 | 13 | 13 |
| Cal6 | 2.91 | 0.092 | 2.40 | 0.138 | 1.2 | 7 | 7 |
| Cal7 | 1.80 | 0.057 | 1.35 | 0.078 | 1.3 | 5 | 4 |
| Cal8 | 2.06 | 0.065 | 1.67 | 0.096 | 1.2 | 6 | 5 |
| Cal9 | 1.73 | 0.055 | 2.16 | 0.124 | 0.8 | 4 | 6 |
| Cal10 | 1.70 | 0.054 | 1.24 | 0.071 | 1.4 | 3 | 3 |
| Cal11 | 4.01 | 0.128 | 3.86 | 0.222 | 1.0 | 9 | 11 |
| Cal12 | 3.73 | 0.118 | 2.55 | 0.147 | 1.5 | 8 | 8 |
| Cal13 | 9.86 | 0.314 | 6.92 | 0.399 | 1.4 | 14 | 14 |
| Cal14 | 5.77 | 0.183 | 4.34 | 0.250 | 1.3 | 12 | 12 |
| ID | AA _{exp} | | AA _{exp m} | | AA _{exp} /AA _{exp m} | | |
| EXP | 31.45 | | 17.37 | | 1.8 | | |

Table 1. Calculation of AA and AA_m for pressurizer pressures in time interval (0–20 s)

| ID | AA _{err} | AA | AA _{err m} | AA _m | AA _{err} / AA _{err m} | Rank AA | Rank AA _m |
|-------|-------------------|-------|---------------------|-----------------|--|---------|-------------------------|
| Cal1 | 3.06 | 0.096 | 3.85 | 0.237 | 0.8 | 8 | 8 |
| Cal2 | 1.08 | 0.034 | 1.23 | 0.076 | 0.9 | 1 | 1 |
| Cal3 | N.A. | N.A. | N.A. | N.A. | N.A. | N.A. | N.A. |
| Cal4 | 3.10 | 0.097 | 3.97 | 0.244 | 0.8 | 9 | 9 |
| Cal5 | 3.93 | 0.123 | 4.96 | 0.305 | 0.8 | 11 | 11 |
| Cal6 | N.A. | N.A. | N.A. | N.A. | N.A. | N.A. | N.A. |
| Cal7 | 1.17 | 0.036 | 1.38 | 0.085 | 0.8 | 3 | 3 |
| Cal8 | 1.49 | 0.047 | 1.80 | 0.111 | 0.8 | 4 | 4 |
| Cal9 | 1.64 | 0.051 | 2.09 | 0.129 | 0.8 | 5 | 5 |
| Cal10 | 1.10 | 0.034 | 1.34 | 0.082 | 0.8 | 2 | 2 |
| Cal11 | 2.97 | 0.093 | 3.74 | 0.230 | 0.8 | 7 | 7 |
| Cal12 | 2.23 | 0.070 | 2.71 | 0.167 | 0.8 | 6 | 6 |
| Cal13 | 5.96 | 0.186 | 7.44 | 0.458 | 0.8 | 12 | 12 |
| Cal14 | 3.80 | 0.119 | 4.47 | 0.275 | 0.8 | 10 | 10 |
| ID | AA _{exp} | | AA _{exp m} | | AA _{exp} /AA _{exp m} | | |
| EXP | 32.00 | | 16.26 | | 2.0 | | |

Table 2. Calculation of AA and AA_m for pressurizer pressures in time interval (0–119.5 s)

for both, the original FFTBM and the improved FFTBM by signal mirroring are shown. It can be seen that the average amplitude of the experimental signal is similar for both time intervals. The reason is that after 20 s the pressure signal (see Fig. 4(a)) is not changing very much. As the pressure at 20 s significantly dropped, the edge effect at 20 s is rather similar

to the edge effect at 119.5 s. The average amplitudes of the experimental signal obtained by the original FFTBM are 1.8 and 2.0 times larger than by the improved FFTBM by signal mirroring for the first and second time interval, respectively. The conclusion for the error signals (see Fig. 4(b)) is different. The ratio of the average amplitudes of the error signal varies between 0.8 and 1.5 in the first time interval, while in the second time interval this ratio is around 0.8. The reason for the varying ratio in the first time interval is that the edges between calculations are quite different, while in the second time interval the edges are rather similar between calculations. Ranking of the AA values may change only in the case when the ratio of AA_{err} varies, i.e. in the first time interval, as it can be seen from Table 1. In the second time interval (in the whole calculation) the rank of AA remains unchanged, as shown in Table 2. Nevertheless, the absolute value of AA changes when the edge is not considered in the experimental signal and this influences the total accuracy.

6.4 Application to single variable

Fig. 5 shows the comparison between experimental and calculated data, the error signals between the calculation and the experiment, AA calculated with the original FFTBM, and AA_m calculated with the improved FFTBM by signal mirroring. For the rod surface temperature shown in Fig. 5(a) the calculated maximum values of the rod surface temperature were in rather good agreement with the experimental value. However, the trends were in general under or over predicted, with some calculations that predicted quench too early. From the error signals shown in Fig. 5(b) it can be seen that discrepancies were present until core quench. From Fig. 5(c) it can be seen that the edge effect is present in the calculation of AA. When looking AA_m in Fig. 5(d) it can be seen that the value of AA_m monotonically increases as long as the discrepancy is present. Nevertheless, when considering the whole transient time interval, there is only a slight difference between AA and AA_m . The reason is the small edge in the whole transient time interval. This is the reason why the original FFTBM in several cases produced reasonable results (but not for monotonically increasing and decreasing signals like the pressurizer pressure). Nevertheless, for investigating the influence of discrepancies as we progress into the transient the edge effect needs to be eliminated to make the right conclusions. Only the improved FFTBM by signal mirroring gives consistent results. Consistent judgment of the time dependent accuracy is very important as the analyst in this way gets an objective picture how each discrepancy decreases the accuracy. On the other hand, from Fig. 5(c) it can be very easily verified that the requirements for accuracy measures (Ambrosini et al., 1990) that at any time into the transient the previous history should be remembered and that the measure should be independent upon the transient duration are not well fulfilled in the case of the original FFTBM when the edge influences the results. Through performing the time dependent accuracy, tens of calculations for different time intervals were performed demonstrating the consistency of the improved FFTBM by signal mirroring comparing to the original FFTBM and therefore there is no need to use further experiments for the validation of the improved FFTBM. On the other hand, very frequently at the end of the transient the edges are rather small and in such cases also the original FFTBM produces consistent results. Luckily, this was the case in several studies performed with the original FFTBM (Prošek et al., 2002). Nevertheless, before the analyst is confident to the results obtained by the original FFTBM he should always verify that the edge is not present in the signal. In the opposite, the results are doubtful. It should be also noted that the methodology using the FFTBM requires qualitative analysis with visual observation and only for

discrepancies which are reasonable and understood the quantitative assessment using FFTBM could be done.

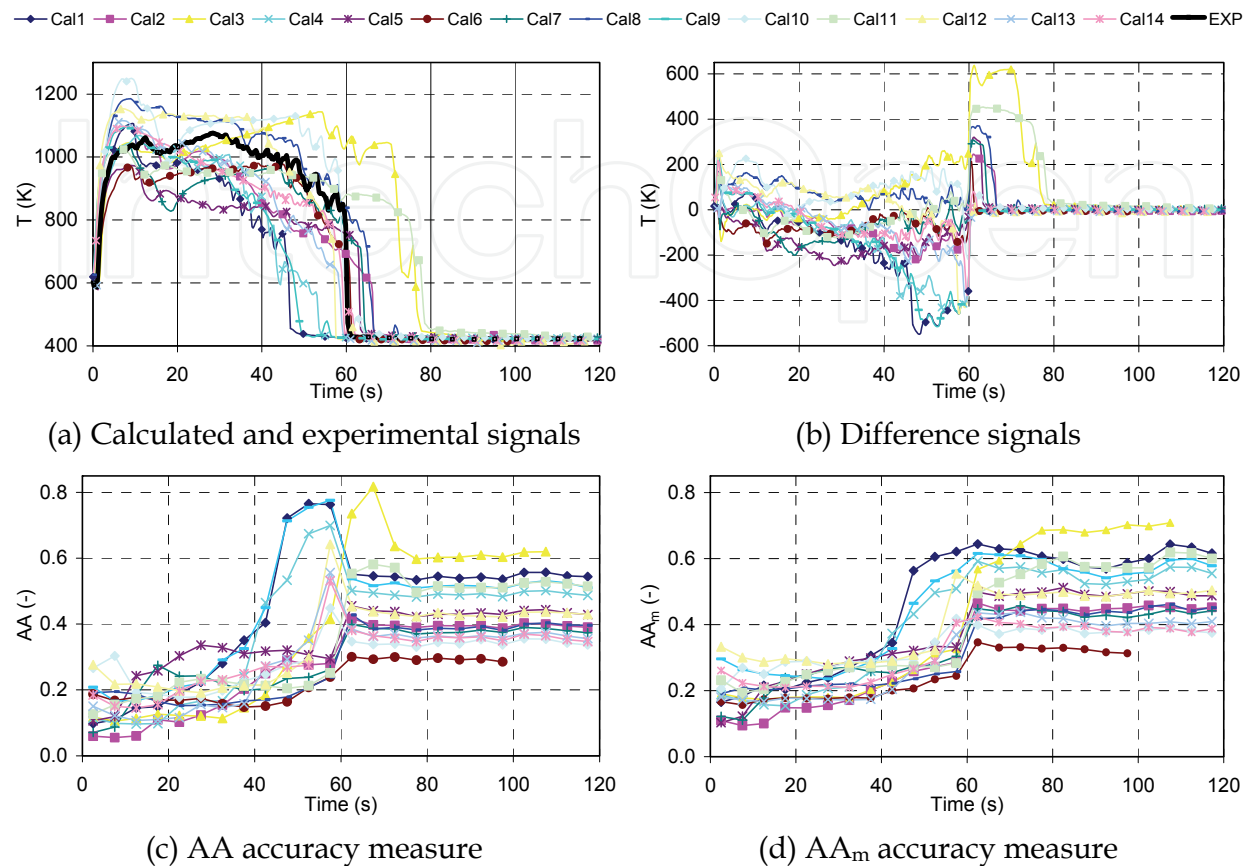


Fig. 5. Results for the LOFT L2-5 test calculations of rod surface temperature

6.5 Accuracy criterion for primary pressure

The differences between AA and AA_m as a function of time were clearly shown to be due to the edge contribution. On the other hand, for the whole transient time interval with stabilized conditions resulting in small edges also the judgment by the original FFTBM is qualitatively correct. However, this is never the case for monotonic trends where the edge increases with increasing the transient time. This can be seen from Fig. 6 showing AA and AA_m for pressurizer pressure shown in Fig. 4. After 20 s the AA value is low due to the large edge present in the experimental signal, which is used for normalization.

Based on the results in Fig. 6 it seems that the restrictive pressure criterion (AA below 0.1) in the original FFTBM was set, because it was based on pressure trends during small break LOCAs in facilities simulating typical PWRs (high initial pressure and large pressure drop after break occurrence, therefore high edge). When tests on different facilities were simulated, there were difficulties in satisfying the primary pressure criterion. The first example is the accuracy quantification of four standard problem exercises (SPEs) organized by IAEA (D'Auria et al., 1996). In this study only the primary system pressure has been considered. Among other things it was also concluded that in the case of SPE-3 the calculation is clearly unacceptable (AA was 0.31) and that more complex transients lead to worse results than simple one's. As no plots are shown in the paper by D'Auria et al. (1996)

no further conclusion can be done except that the pressure drop (edge) is smaller than in a typical PWR. Namely, the initial pressure in this test is lower than in the typical PWR test. By lowering the pressure edge the values of AA are increased. This can be still better illustrated in the recent application of FFTBM to heavy water reactors. In the study (Prošek et al., 2006) all participants fulfilled the acceptance criterion for the total accuracy $K < 0.4$ while the primary pressure criterion was not fulfilled. In the blind accuracy calculation the AA value for the primary pressure was 0.117 for the best calculation. The header 7 pressure with initial pressure around 10 MPa was selected as a variable representing the primary pressure. In the open accuracy analysis header 6 pressure was proposed by a representative from Italy. The initial value of this pressure was around 12 MPa. Now the value of AA was below 0.1 for most of participants mostly due to the increased pressure edge effect (the best AA was 0.074) due to the higher pressure.

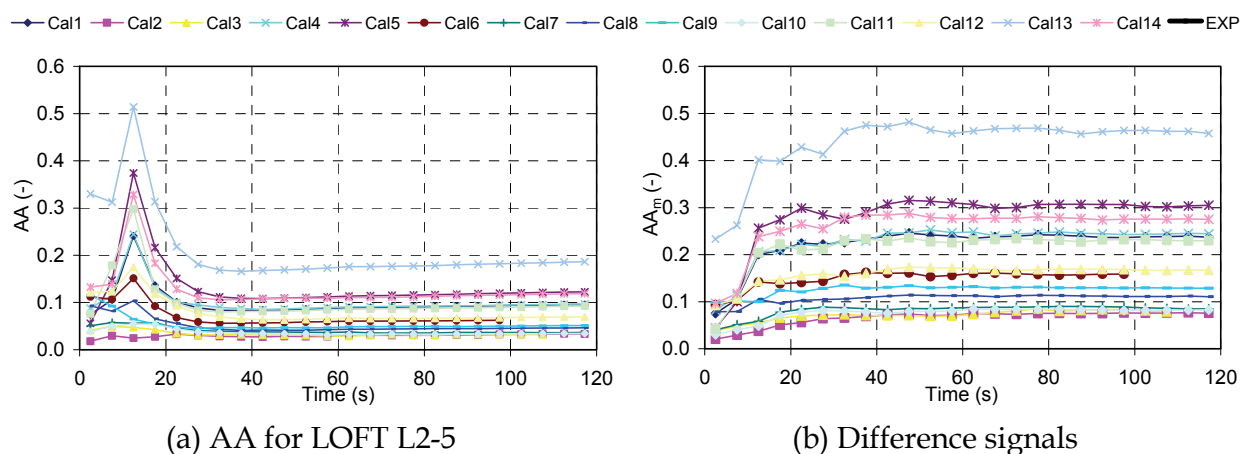


Fig. 6. Accuracy measures for the LOFT L2-5 test calculations of pressurizer pressure

The last example of the AA calculation for the primary pressure is for ISP-22 calculations (loss of feedwater test). From paper by Prošek et al. (2002) it may be seen that the AA value for the primary pressure in the best posttest calculation is 0.21, the worst (as judged by the original FFTBM) among summarized ISPs. From the original report (Ambrosini et al., 1992) showing plots it can be easily concluded that the edge contribution in the experimental signal is smaller than typically for small break LOCAs due to lower pressure drop and the complex shape of the experimental signal, resulting in larger AA.

All these examples demonstrate that due to the unpredictable edge contribution a consistent criterion for the primary pressure cannot be defined for the original FFTBM, while for the improved FFTBM with signal mirroring this can be done.

6.6 Moving average

When trends oscillate greatly (e.g., the steam generator pressure drops shown in Fig. 7), special treatment is needed (Prošek & Mavko, 2009). To correctly reproduce the experimental signal by linear interpolation, many points are needed. This is achieved by increasing the maximum frequency component of the signal. However, it makes no sense to increase the number of points, as some cases have a sampling frequency 30 times larger than the calculated data. When many points are used, the main contribution to the amplitude spectrum comes from the oscillations (very often noise) in the experimental

signal for which the calculated data have no information. The correct procedure is therefore to smooth the data. Smoothing data removes random variations and shows trends and cyclic components. The simplest way to smooth the data is by taking the averages. This is done by use of the moving average of the experimental signal. Mathematically, the moving average is an example of a convolution of the input signal with a rectangular pulse having an area of 1.

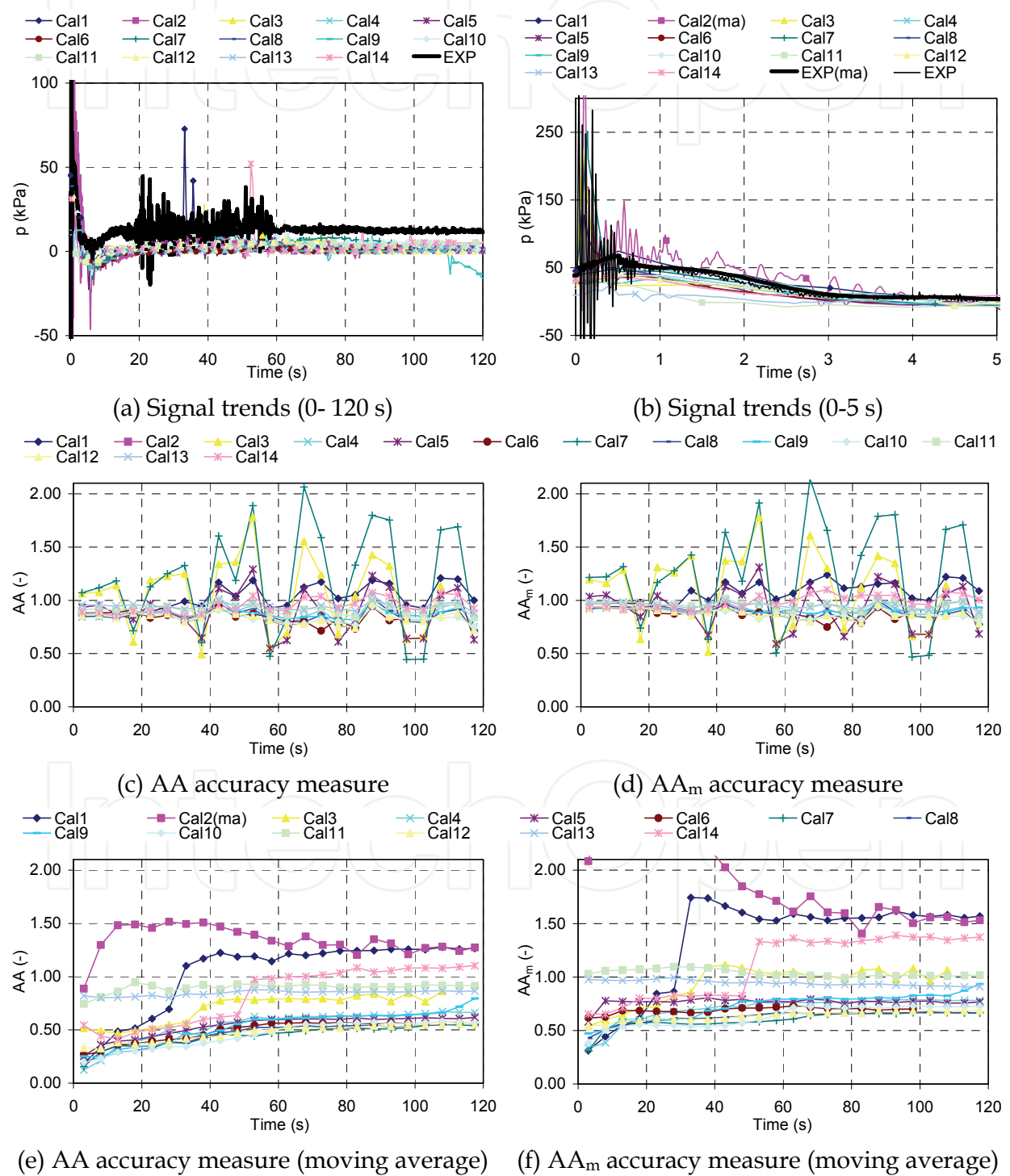


Fig. 7. Results for the LOFT L2-5 test calculations of steam generator pressure drop

Without using the moving average, AA varies around a certain value. In the presented case for steam generator pressure drop, the values of AA and AA_m are close to 1 (see Figs. 7(c) and 7(d)), because the calculated values are much smaller than the experimental values. The exception is Cal2 which values vary around 4 and is not visible in Figs. 7(c) and 7(d). Variations in AA are the consequence of inappropriately prepared experimental data for the FFTBM analysis. The problem of the oscillatory signal was less significant in the past, because the original FFTBM limited the number of data points to 1,000, and data reduction was needed when this value was exceeded. Thus, data reduction is another possibility to use for partially smoothing the signal and thereby increasing the accuracy by eliminating some noise. However, as shown by Figure 4(e) in Prošek et al., 2006, the AA still varies because the moving average was not used. The reason is that, by increasing the time interval and not increasing the number of points, the amplitude spectrum changes as the signal between two consecutive data points is not a monotonic function (it oscillates). This gives a different amplitude spectrum of the experimental and difference signal. When moving average was used in the case of the steam generator pressure drop experimental signal, the AA values no longer oscillate in phase because of AA_{exp} , as shown in Figs. 7(e) and 7(f). This suggests that the observation of oscillations being in phase in the calculated AAs indicates that moving average should be used. Figures 7(e) and 7(f) show a sudden increase in AA in the Cal1 and Cal5 calculations. The reason for this increase are the pressure spikes clearly shown in Fig. 7(a). Each spike significantly deteriorates the results. Finally, FFTBM was able to detect the deviation in the Cal9 calculation at the end of the transient.

Another important finding is that the mismatch between the experimental data and the calculations for the steam generator pressure drop variable is present from the very beginning of the transient, as shown in Fig. 7(b). Only the Cal2 calculation reproduced the frequency of oscillations in the first second. However, because the peaks were too high, the calculation was not very accurate. Use of moving average removes the large oscillations from the experimental signal (EXP(ma)), while in the Cal2(ma) calculation, the oscillations still remain in the beginning of the transient. Later (at approximately 15 seconds), the pressure drop stabilizes and the values oscillate around their mean values. This means that the transient related to the pressure drop has more or less ended.

6.7 Comparison of results obtained by FFTBM and ACAP

Tables 3 and 4 shows the comparison of FFTBM and Automated Code Assessment Program (ACAP) (Kunz et al., 2002) accuracy measures for the calculated pressurizer pressure and rod surface temperature shown in Figs. 4 and 5, respectively. This comparison was made for the independent assessment that FFTBM provides for consistent accuracy measures. The calculations are sorted according to AA_m in ascending manner. For the pressurizer pressure it can be seen that AA_m , AA, mean square error (MSE), and cross-correlation coefficient (XCC) accuracy measures agree well. The only difference is that MSE and XCC indicate that all calculations of pressurizer pressure are very good, while FFTBM shows that some are not so accurate and some do not even fulfil the original FFTBM primary pressure criterion. As the pressure criterion was developed without consideration of the edge effect, care must be taken in its use, as indicated by the ACAP results. Finally, D'Auria fast Fourier transform (DFFT) and continuous wavelet transform (CWT) accuracy measures do not help much in this case.

| Method | FFTBM | | ACAP | | | |
|--------------|-----------------|-------|-------|-------|-------|-------|
| Calculation | AA _m | AA | DFFT | MSE | XCC | CWT |
| Cal6 (100 s) | 0.076 | 0.034 | 0.194 | 1.000 | 1.000 | 0.154 |
| Cal10 | 0.079 | 0.032 | 0.132 | 1.000 | 0.999 | 0.008 |
| Cal14 | 0.082 | 0.034 | 0.173 | 1.000 | 0.999 | 0.116 |
| Cal13 | 0.085 | 0.036 | 0.223 | 1.000 | 0.999 | 0.059 |
| Cal7 | 0.111 | 0.047 | 0.173 | 0.999 | 0.999 | 0.148 |
| Cal8 | 0.129 | 0.051 | 0.194 | 1.000 | 0.999 | 0.179 |
| Cal2 | 0.159 | 0.062 | 0.168 | 0.999 | 0.999 | 0.008 |
| Cal5 | 0.167 | 0.070 | 0.134 | 0.998 | 0.997 | 0.126 |
| Cal12 | 0.230 | 0.093 | 0.082 | 0.998 | 0.993 | 0.006 |
| Cal4 | 0.237 | 0.096 | 0.129 | 0.998 | 0.994 | 0.140 |
| Cal9 | 0.244 | 0.097 | 0.128 | 0.998 | 0.995 | 0.220 |
| Cal11 | 0.275 | 0.119 | 0.110 | 0.997 | 0.992 | 0.069 |
| Cal1 | 0.305 | 0.123 | 0.089 | 0.996 | 0.983 | 0.091 |
| Cal3 (110 s) | 0.458 | 0.186 | 0.096 | 0.991 | 0.972 | 0.053 |

Table 3. Comparison of FFTBM and ACAP accuracy measures for pressurizer pressure in time interval (0–119.5 s)

| Method | FFTBM | | ACAP | | | |
|--------------|-----------------|-------|-------|-------|-------|-------|
| Calculation | AA _m | AA | DFFT | MSE | XCC | CWT |
| Cal6 (100 s) | 0.313 | 0.285 | 0.245 | 0.989 | 0.992 | 0.020 |
| Cal10 | 0.375 | 0.337 | 0.197 | 0.984 | 0.987 | 0.193 |
| Cal14 | 0.388 | 0.347 | 0.228 | 0.988 | 0.973 | 0.171 |
| Cal13 | 0.409 | 0.356 | 0.206 | 0.982 | 0.960 | 0.106 |
| Cal7 | 0.442 | 0.374 | 0.203 | 0.983 | 0.968 | 0.006 |
| Cal8 | 0.451 | 0.396 | 0.182 | 0.980 | 0.972 | 0.010 |
| Cal2 | 0.452 | 0.391 | 0.208 | 0.982 | 0.962 | 0.055 |
| Cal5 | 0.488 | 0.429 | 0.181 | 0.968 | 0.962 | 0.055 |
| Cal12 | 0.504 | 0.429 | 0.207 | 0.981 | 0.967 | 0.004 |
| Cal4 | 0.555 | 0.487 | 0.158 | 0.948 | 0.883 | 0.043 |
| Cal9 | 0.578 | 0.511 | 0.150 | 0.938 | 0.853 | 0.049 |
| Cal11 | 0.600 | 0.515 | 0.152 | 0.940 | 0.832 | 0.000 |
| Cal1 | 0.616 | 0.544 | 0.151 | 0.929 | 0.841 | 0.055 |
| Cal3 (110 s) | 0.708 | 0.620 | 0.149 | 0.901 | 0.780 | 0.000 |

Table 4. Comparison of FFTBM and ACAP accuracy measures for rod surface temperature (i.e. rod cladding temperature) in time interval (0–119.5 s)

For rod surface temperature (see Table 4), AA_m, AA, MSE, and XCC accuracy measures agree well. The XCC figure of merit is in especially good agreement with AA_m. When comparing the Cal12 and Cal13 calculations, FFTBM slightly favours the Cal13 calculation, while ACAP gives comparable values. The qualitative analysis of dryout occurrence reported in Table 13 of the BEMUSE Phase II Report (OECD/NEA, 2006) showed, that the Cal13 calculation receives three excellent and one minimal mark, while the Cal12 calculation

receives two excellent, one reasonable, and one minimal mark. One parameter representing the dryout occurrence is the peak cladding temperature and for it the Cal13 calculation is qualitatively judged better than the Cal12 calculation. These BEMUSE results support the FFTBM judgments for cladding temperature. Examination of AA_m in Fig. 5(d) shows that, in the initial period of 40 seconds, the Cal13 calculation is significantly better because of the Cal12 calculation's large overprediction of cladding temperature.

6.8 Discussion

A demonstration application of the improved FFTBM by signal mirroring was done for a design basis accident. In the case of the LOFT L2-5 test calculation it was shown that only the improved FFTBM by signal mirroring gives a realistic judgment for the time dependent accuracy. The differences between AA and AA_m as a function of time were clearly shown to be due to the edge contribution. On the other hand, for the whole transient time interval with stabilized conditions resulting in small edges also the judgment by the original FFTBM is qualitatively correct. However, this is never the case for monotonic trends where the edge increases with increasing the transient time.

In general there is a need to make comparisons for any time window and the transient may not be terminated at stable conditions resulting in small edges. For the proposed improved FFTBM by signal mirroring the acceptability criteria need to be defined in the same way as this was done for the original FFTBM. The easiest way would be to use the same set of calculations as for the original FFTBM. The obtained results for LOFT L2-5 suggest slightly higher acceptability limits for the improved FFTBM by signal mirroring than for the original FFTBM, including the restrictive pressure criterion.

7. Conclusions

In the past the most widely used method for code accuracy quantification of primary system thermal-hydraulic codes was the original FFTBM. Recently, in the original FFTBM an important deficiency was discovered. It turned out that the accuracy measure depends on the difference between the first and last data point of the investigated signal. Namely, the DFT mathematical method, on which the FFTBM is based, treats the investigated finite length signal as an infinite length periodic signal, introducing discontinuities if the first and last data point of the finite signal differ. These discontinuities produce a variegated spectrum of frequencies when applying DFT, which may overshadow the frequency spectrum of the investigated signal. This so called edge effect is a significant deficiency of the original FFTBM since for the comparison the shape of the investigated signal is important and not the artificially introduced unphysical edge.

Therefore the authors proposed to resolve the edge effect problem on a unique way by signal mirroring, where the investigated signal is mirrored before FFTBM is applied. By composing the original signal and its mirrored signal a symmetric signal with the same characteristics is obtained, but without introducing artificial discontinuities when viewed as a periodically extended infinite signal. With the so improved FFTBM by signal mirroring a consistent and unbiased tool for quantitative assessment is obtained. An additional good property of the improved FFTBM is that the same FFTBM procedure (numerical tools etc.) may be applied as with the original FFTBM.

The benefits of the improved FFTBM by signal mirroring were demonstrated on the large break LOCA test LOFT L2-5. The results show that the so improved FFTBM judges the

accuracy of variables in a reliable, unbiased and consistent way. Nevertheless, the new measure for indication of the time shift between the experimental and the calculated signal can be used only by the original FFTBM. It is also suggested to make all operations in the time domain for both, the original and the improved FFTBM, as it is very difficult to make adjustments in the frequency domain (e.g. logarithmic scale, moving average). There is no way to make such adjustments automatically. Finally, it should not be forgotten, that the qualitative analysis is a prerequisite to perform the quantitative analysis. This means that thermal hydraulic code calculations must be analyzed by experts first, and only then FFTBM can assist in conducting an objective comparison and answering if improvements to the input model are needed.

8. References

- Aksan, S.N., D'Auria, F. & Bonato, S. (2001). Application of Fast Fourier Transform Based Method (FFTBM) to the results of ISP-42 PANDA test calculations: Phase A. *Proceedings of the ICONE-9*, April 8-12, 2001, Nice, France.
- Ambrosini, W., Bovalini, R. & D'Auria, F. (1990). Evaluation of accuracy of thermalhydraulic code calculations. *Energia Nucleare*, 7, 2 (May-September 1990), 5-16.
- Ambrosini, W., Breggi, M.P., D'Auria, F. & Galassi, G.M. (1992). Evaluation of post-test analyses of OECD-CSNI International Standard Problem 22. Report, University of Pisa, NT 184 (91) Rev.1.
- D'Auria, F. & Galassi, M. (1997). Accuracy Quantification by the FFT method in FARO L-14 (ISP 39) open calculations, University of Pisa, NT 309(97).
- D'Auria, F., Eramo, A., Frogheri, M. & Galassi, G.M. (1996). Accuracy quantification in SPE-1 to SPE-4 organised by IAEA. *Proc. Int. Conf. on Nucl. Engineering (ICONE-4)*, Vol. 3, pp. 461-469, ISBN 0-7918-1226-X, New Orleans, Louisiana, March 10-14, 1996.
- D'Auria, F., Oriolo, F., Leonardi, M. & Paci, S. (1995). Code Accuracy Evaluation of ISP35 Calculations Based on NUPEC M-7-1 Test. *Proc. Second Regional Meeting: Nuclear Energy in Central Europe*, pp. 516-523. ISBN 961-900004-9-8, Portorož, Slovenia, September 2005, Nuclear Society of Slovenia, Ljubljana.
- D'Auria, F., Leonardi, M. & Pochard, R. (1994). Methodology for the evaluation of thermalhydraulic codes accuracy. *Proc. Int. Conf. on New trends in Nuclear System Thermohydraulics*, pp. 467-477, Pisa, Italy, May 2004, Edizioni ETS Pisa.
- Kunz, R.F., Kasamala, G.F., Mahaffy, J.H. & Murray, C.J. (2002). On the automated assessment of nuclear reactor systems code accuracy. *Nuclear Engineering and Design*, 211, 2-3 (February 2002), 245-272, ISSN 0029-5493.
- Mavko, B., Prošek, A. & D'Auria, F. (1997). Determination of code accuracy in predicting small-break LOCA experiment. *Nuclear Technology*, 120, 1, (October 1997), 1-19, ISSN 0029-5450.
- OECD/NEA (2006). BEMUSE Phase 2 Report: Re-Analysis of the ISP-13 Exercise, Post Test Analysis of the LOFT L2-5 Test Calculation. OECD/NEA Report, Committee on the Safety of Nuclear Installations (CSNI), NEA/CSNI/R(2006)2.
- Prošek, A. & Leskovar, M. (2009). Extensions of the fast Fourier transform based method for quantitative assessment of code calculations. *Electrotechnical Review*, 76, 5 (December 2009), 251-256, ISSN 0013-5852, (<http://ev.fe.uni-lj.si/5-2009/Prosek.pdf>).

- Prošek, A. & Mavko, B. (2003). A tool for quantitative assessment of code calculations with an improved fast Fourier transform based method. *Electrotechnical Review*, 70, 5 (December 2003), 291–296, ISSN 0013-5852, (<http://ev.fe.uni-lj.si/5-2003/prosek.pdf>).
- Prošek, A. & Mavko, B. (2009). Quantitative code assessment with fast Fourier transform based method improved by signal mirroring, (International agreement report, NUREG/IA-0220). Washington: U. S. NRC (<http://www.nrc.gov/reading-rm/doc-collections/nuregs/agreement/ia0220/ia0220.pdf>).
- Prošek, A., D'Auria, F., Richards, D.J. & Mavko, B. (2006). Quantitative assessment of thermal-hydraulic codes used for heavy water reactor calculations. *Nuclear Engineering and Design*, 236, 3 (February 2006), 295–308, ISSN 0029-5493.
- Prošek, A., D'Auria, F. & Mavko, B. (2002). Review of quantitative accuracy assessments with fast Fourier transform based method (FFTBM). *Nuclear Engineering and Design*, 217, 1-2 (August 2002), 179-206, ISSN 0029-5493.
- Prošek, A., Leskovar, M. & Mavko, B. (2008). Quantitative assessment with improved fast Fourier transform based method by signal mirroring. *Nuclear Engineering and Design*, 238, 10 (October 2008), 2668-2677, ISSN 0029-5493. (Figs. 1, 3, 4, 5, 6 and Tables 1, 2 Reprinted from *Nuclear Engineering and Design*, Volume 238, Issue 10, A. Prošek, M. Leskovar, B. Mavko, Pages 2668-2677, Copyright (2010), with permission from Elsevier.)
- Smith S. W. (1999). *The Scientist and Engineer's Guide to Digital Signal Processing*, Second Edition, California Technical Publishing, ISBN 0-9660176-7-6, San Diego, California.
- Szabados, L., Ézsöl, Gy., Perneczky, L., Tóth, I., Guba, A., Takács, A. & Trosztel, I. (2009). *Volume II. Major findings of PMK-2 Test Results and Validation of thermohydraulic System Codes for VVER Safety Studies*, Akadémiai Kiadó, ISBN 978-963-05-8810-2, Budapest, Hungary.

IntechOpen



Fourier Transforms - Approach to Scientific Principles

Edited by Prof. Goran Nikolic

ISBN 978-953-307-231-9

Hard cover, 468 pages

Publisher InTech

Published online 11, April, 2011

Published in print edition April, 2011

This book aims to provide information about Fourier transform to those needing to use infrared spectroscopy, by explaining the fundamental aspects of the Fourier transform, and techniques for analyzing infrared data obtained for a wide number of materials. It summarizes the theory, instrumentation, methodology, techniques and application of FTIR spectroscopy, and improves the performance and quality of FTIR spectrophotometers.

How to reference

In order to correctly reference this scholarly work, feel free to copy and paste the following:

Andrej Prošek and Matjaž Leskovar (2011). Application of Fast Fourier Transform for Accuracy Evaluation of Thermal-Hydraulic Code Calculations, Fourier Transforms - Approach to Scientific Principles, Prof. Goran Nikolic (Ed.), ISBN: 978-953-307-231-9, InTech, Available from: <http://www.intechopen.com/books/fourier-transforms-approach-to-scientific-principles/application-of-fast-fourier-transform-for-accuracy-evaluation-of-thermal-hydraulic-code-calculations>

INTECH
open science | open minds

InTech Europe

University Campus STeP Ri
Slavka Krautzeka 83/A
51000 Rijeka, Croatia
Phone: +385 (51) 770 447
Fax: +385 (51) 686 166
www.intechopen.com

InTech China

Unit 405, Office Block, Hotel Equatorial Shanghai
No.65, Yan An Road (West), Shanghai, 200040, China
中国上海市延安西路65号上海国际贵都大饭店办公楼405单元
Phone: +86-21-62489820
Fax: +86-21-62489821

© 2011 The Author(s). Licensee IntechOpen. This chapter is distributed under the terms of the [Creative Commons Attribution-NonCommercial-ShareAlike-3.0 License](https://creativecommons.org/licenses/by-nc-sa/3.0/), which permits use, distribution and reproduction for non-commercial purposes, provided the original is properly cited and derivative works building on this content are distributed under the same license.

IntechOpen

IntechOpen